Anal. Chem. **2010,** *82,* 7302–7308

Atmospheric Pressure-Ion Drift Chemical Ionization Mass Spectrometry for Detection of Trace Gas Species

Jun Zheng, Alexei Khalizov, Lin Wang, and Renyi Zhang*

Departments of Chemistry and Atmospheric Sciences, Texas A & M University, College Station, Texas 77843-3150

This paper describes atmospheric pressure-ion drift chemical ionization mass spectrometry (AP-ID-CIMS) for monitoring of ambient trace species. Operation of the drift tube at atmospheric pressure allows a significantly longer ion−molecule reaction time and eliminates dilution of the ambient samples, while a well-defined electric field inside the drift tube provides the benefits to confine the flight path and velocity of reagent/product ions, to break down ion clusters, and to control the ion−molecule reaction time. The AP-ID-CIMS exhibits advantages over the conventional low pressure ID-CIMS and flow tube AP-CIMS, improving the detection sensitivity by 3 orders of magnitude and a factor of 3, respectively. We demonstrate that the AP-ID-CIMS allows quantification of sulfuric acid concentrations and is capable of detecting gaseous sulfuric acid with a detection limit of less than 10^5 molecules cm^{-3}, on the basis of 3σ of the baseline noise and an integration time of 12 s. A field evaluation of the AP-ID-CIMS is presented for ambient H_2SO_4 measurements.

Since the first introduction of chemical ionization mass spectrometry (CIMS) by Munson and Field,[1] CIMS has been widely employed in the field of analytical chemistry, mainly because of its less fragmented and thus more informative mass spectra. In contrast to the more energetic ionization methods, such as electron impact (EI), CIMS employs gas-phase ion−molecule reactions to ionize neutral analytes. Application of CIMS in atmospheric trace gas detection stemmed from the ion composition measurements in the troposphere and stratosphere.[2−5] In particular, ion−molecule reaction schemes naturally occurring in the atmosphere[5] were utilized with the CIMS techniques for in situ detection of neutral species, such as gaseous nitric acid (HNO_3)[6] and sulfuric acid (H_2SO_4)[7] with concentrations from several parts per billion by volume (ppbv) to 0.01 parts per trillion by volume (pptv) in the atmosphere.

One of the most successful developments of CIMS in atmospheric chemistry studies is the introduction of proton transfer reaction-mass spectrometry (PTR-MS),[8,9] which utilizes the hydronium ion ($H_3{}^+O$) to protonate an analyte with a proton affinity higher than water. The success of PTR-MS stems from the concept of combining CIMS and a flow-drift tube (FDT) configuration[10] that enables the less exothermic proton transfer reactions under controllable ion−molecule reaction conditions. Currently, PTR-MS has been exclusively utilized to measure volatile organic compounds (VOCs) in the laboratory and in the atmosphere with a detection limit as low as a few pptv.[11−14] FDT was originally designed for studies of ion−molecule reaction kinetics, such as the measurements of ion−molecule reaction rate constants and ion mobilities.[15] The unique feature of FDT is that it acts as ion optics to confine and constrain the ion movement through a well-defined electric field. For example, Eisele[16] implemented a counter FDT device to preconcentrate naturally occurring ions during atmospheric ion composition measurements by slowing down ions movement in the sample inlet. In the case of PTR-MS, a FDT is used to control, usually speed up, reagent ion velocity so that the ion−molecule reaction time is limited to be less than 1 ms. When the H_3O^+ concentration is far greater than that of product ions, the analyte concentration can be calculated from

$$[RH^+] = [H_3O^+][R]k_p t_p \qquad \text{(E1)}$$

where $[RH^+]$ is the product ions intensity, $[H_3O^+]$ is the intensity of hydronium ions, [R] is the neutral analyte concentration, k_p is the proton-transfer reaction rate constant,[17] and t_p is the reaction time. Because the kinetic energy of ions increases substantially under the influence of the electric field (typically ~120 Td, 1 Td = 10^{-17} V cm^2), weakly bounded water

* To whom correspondence should be addressed.

(1) Munson, M. S. B.; Field, F. H. *J. Am. Chem. Soc.* **1966**, *88*, 2621–2630.
(2) Arnold, F.; Henschen, G. *Nature* **1978**, *275*, 521–522.
(3) Arnold, F.; Krankowsky, D.; Marien, K. H. *Nature* **1977**, *267*, 30–32.
(4) Eisele, F. L. *J. Geophys. Res.* **1986**, *91*, 7897–7906.
(5) Viggiano, A. A. *Mass Spectrom. Rev.* **1993**, *12*, 115–137.
(6) Mohler, O.; Arnold, F. *J. Atmos. Chem.* **1991**, *13*, 33–61.
(7) Arnold, F.; Fabian, R. *Nature* **1980**, *283*, 55–57.
(8) Hansel, A.; Jordan, A.; Holzinger, R.; Prazeller, P.; Vogel, W.; Lindinger, W. *Int. J. Mass Spectrom.* **1995**, *149*, 609–619.
(9) Lindinger, W.; Hansel, A.; Jordan, A. *Int. J. Mass Spectrom.* **1998**, *173*, 191–241.
(10) McFarlan, M.; Albritto, Dl.; Fehsenfe, Fc.; Ferguson, E. E.; Schmelte, Al. *J. Chem. Phys.* **1973**, *59*, 6610–6619.
(11) Blake, R. S.; Monks, P. S.; Ellis, A. M. *Chem. Rev.* **2009**, *109*, 861–896.
(12) de Gouw, J.; Warneke, C. *Mass Spectrom. Rev.* **2007**, *26*, 223–257.
(13) Zhao, J.; Zhang, R. Y.; Fortner, E. C.; North, S. W. *J. Am. Chem. Soc.* **2004**, *126*, 2686–2687.
(14) Zhao, J.; Zhang, R. Y.; Misawa, K.; Shibuya, K. *J. Photochem. Photobiol. A* **2005**, *176*, 199–207.
(15) Mason, E. A.; McDaniel, E. W. *Transport Properties of Ions in Gases*; Wiley: New York, 1988.
(16) Eisele, F. L. *Int. J. Mass Spectrom. Ion Processes* **1983**, *54*, 119–126.
(17) Zhao, J.; Zhang, R. Y. *Atmos. Environ.* **2004**, *38*, 2177–2185.

10.1021/ac101253n
Published on Web 08/09/2010

clusters (e.g., $H_3O^+ \cdot (H_2O)_{n=1,2,...}$) are readily broken down because of collisions with the buffer gas (N_2 or O_2).

Fortner et al.[18] developed an ion drift - chemical ionization mass spectrometer (ID-CIMS) that combines the technique of FDT and the traditional CIMS, which has been widely used for detection of various reactive organic and inorganic species.[5,19−24] ID-CIMS possesses the similar advantages as PTR-MS, but expands the range of detectable species well beyond VOCs. In laboratory studies, ID-CIMS has been used to measure the kinetics and mechanisms of homogeneous and heterogeneous reactions of various atmospherically relevant inorganic and organic compounds.[13,14,25,26] It has been demonstrated that ID-CIMS allows quantification of atmospheric trace nitrogen-containing species (HNO_3 and N_2O_5) without the necessity of in situ calibrations during atmospheric field measurements.[27] Despite the advantage of fast-responding, the detection limit of ID-CIMS is limited by its relatively low operating pressure (~3 Torr). Inside the drift tube the analyte number concentration is diluted by a factor of over 250 after expanding from atmospheric pressure down to a few torr. Furthermore, under a low drift tube pressure the velocity of reagent ions is on the order of 10^3 m s^{-1}, limiting the ion−molecule reaction time to be less than 0.1 ms. For a typical reagent ion intensity of 10^6−10^7 counts per second (cps or Hz), the low-pressure ID-CIMS cannot satisfy the requirement for detection of sub-pptv level of trace gases in the atmosphere, such as gaseous H_2SO_4.

Gaseous H_2SO_4 in the atmosphere is mainly formed from SO_2 oxidation initiated by OH radicals in the presence of oxygen and water vapor. Typical ambient H_2SO_4 mixing ratio varies from 10^5 to 10^7 molecules cm^{-3} (refs 7, 28, and 29). Because liquid H_2SO_4 has a very low saturation vapor pressure under ambient temperature (3.6×10^{-11} Torr at 293 K)[30,31] and its hydration reaction is extremely exothermic, H_2SO_4 has been recognized to play a critical role during new particle formation in the atmosphere.[32−36] In addition, H_2SO_4 contributes to the growth of newly formed particles in a sulfur-rich environment.[37,38] Furthermore, H_2SO_4 condenses readily onto existing particle surface and permanently alters their morphology and optical properties, especially for soot particles.[39−41] H_2SO_4 processed soot aerosols become hydrophilic to act as cloud condensation nuclei (CCN) and thus affect the cloud droplet number concentration and their physical and chemical properties, playing a key role in regulating the Earth energy budget.[42−44]

Because of its essential role in the aerosol chemistry, accurate measurement of the H_2SO_4 concentration is of critical importance. In situ detection of H_2SO_4 by atmospheric pressure chemical ionization mass spectrometry has been used in laboratory and field measurements.[28,29,32,36,38] However, the accuracy in quantifying H_2SO_4 concentration by currently available techniques is still believed to represent the major cause of significant discrepancies among previous studies, especially in the determination of the critical cluster size and threshold H_2SO_4 concentration during nucleation events.[38] The development of a new, reliable technique to improve the accuracy in H_2SO_4 measurements is of special interest to the aerosol science community.

In this paper, we demonstrate that the operation of an ion drift tube at atmospheric pressure significantly improves the detection capabilities of CIMS. Using gaseous H_2SO_4 detection as an example, we show an improvement of several orders of magnitude in the detection limit over the conventional ID-CIMS.[18] In addition, a new H_2SO_4 calibration device is developed to perform multiple-point calibration to illustrate the AP-ID-CIMS methodology. A field evaluation is performed to validate the performance of the AP-ID-CIMS.

EXPERIMENTAL SECTION

Instrument Design. Figure 1 presents a schematic diagram of the AP-ID-CIMS, consisting of a turbulence-reducing inlet, an α-particle (Am-241) radioactive ion source, an atmospheric pressure ion drift tube, a collision-induced dissociation chamber (CID) operating at an intermediate pressure (0.6 Torr), and a quadrupole mass spectrometer. To reduce loss of species on the inlet surface, a 4-in. i.d. 1-ft long aluminum tube is used for the sampling inlet. In addition, the front end of the inlet is machined into a scoop-shape to reduce turbulence-induced wall loss. Typically, ~1200 standard liters per minute (slpm) of ambient air are pulled by a blower (AMETEK Inc., ROTRON 116637) into the inlet at a center-of-flow velocity of about 2.5 m s^{-1}. A cone-shaped mesh is installed to prevent the formation of a stagnant zone at the end

(18) Fortner, E. C.; Zhao, J.; Zhang, R. Y. *Anal. Chem.* **2004**, *76*, 5436–5440.
(19) Huey, L. G. *Mass Spectrom. Rev.* **2007**, *26*, 166–184.
(20) Molina, M. J.; Molina, L. T.; Zhang, R. Y.; Meads, R. F.; Spencer, D. D. *Geophys. Res. Lett.* **1997**, *24*, 1619–1622.
(21) Suh, I.; Lei, W. F.; Zhang, R. Y. *J. Phys. Chem. A* **2001**, *105*, 6471–6478.
(22) Zhang, R. Y.; Leu, M. T.; Keyser, L. F. *Geophys. Res. Lett.* **1995**, *22*, 1493–1496.
(23) Zhang, R. Y.; Leu, M. T.; Keyser, L. F. *J. Phys. Chem.* **1996**, *100*, 339–345.
(24) Zhang, R. Y.; Suh, I.; Lei, W.; Clinkenbeard, A. D.; North, S. W. *J. Geophys. Res.* **2000**, *105*, 24627–24635.
(25) Zhao, J.; Levitt, N. P.; Zhang, R. Y. *Geophys. Res. Lett.* **2005**, *32*.
(26) Zhao, J.; Levitt, N. P.; Zhang, R. Y.; Chen, J. M. *Environ. Sci. Technol.* **2006**, *40*, 7682–7687.
(27) Zheng, J.; Zhang, R.; Fortner, E. C.; Volkamer, R. M.; Molina, L.; Aiken, A. C.; Jimenez, J. L.; Gaeggeler, K.; Dommen, J.; Dusanter, S.; Stevens, P. S.; Tie, X. *Atmos. Chem. Phys.* **2008**, *8*, 6823–6838.
(28) Eisele, F. L.; Tanner, D. J. *J. Geophys. Res.* **1993**, *98*, 9001–9010.
(29) Tanner, D. J.; Eisele, F. L. *J. Geophys. Res.* **1995**, *100*, 2883–2892.
(30) Perry, R. H.; Green, D. W. *Perry's Chemical Engineers' Handbook*, 7th ed.; McGraw-Hill: New York, 1997.
(31) Zhang, R.; Wooldridge, P. J.; Abbatt, J. P. D.; Molina, M. J. *J. Phys. Chem.* **1993**, *97*, 7351–7358.
(32) Benson, D. R.; Young, L. H.; Kameel, F. R.; Lee, S. H. *Geophys. Res. Lett.* **2008**, *35*, 6.
(33) Holmes, N. S. *Atmos. Environ.* **2007**, *41*, 2183–2201.
(34) Zhang, R. *Science* **2010**, *328*, 1366–1367.
(35) Zhao, J.; Khalizov, A. F.; Zhang, R.; McGraw, R. *J. Phys. Chem.* **2009**, *113*, 680–689.
(36) Zhang, R. Y.; Suh, I.; Zhao, J.; Zhang, D.; Fortner, E. C.; Tie, X. X.; Molina, L. T.; Molina, M. J. *Science* **2004**, *304*, 1487–1490.
(37) Yue, D. L.; Hu, M.; Zhang, R.; Wang, Z. B.; Zheng, J.; Wu, Z. J.; Wiedensohler, A.; He, L. Y.; Huang, X. F.; Zhu, T. *Atmos. Chem. Phys.* **2010**, *10*, 4953–4960.
(38) Zhang, R. Y.; Wang, L.; Khalizov, A. F.; Zhao, J.; Zheng, J.; McGraw, R. L.; Molina, L. T. *Proc. Natl. Acad. Sci. U.S.A.* **2009**, *106*, 17650–17654.
(39) Cheng, Y. F.; Berghof, M.; Garland, R. M.; Wiedensohler, A.; Wehner, B.; Muller, T.; Su, H.; Zhang, Y. H.; Achtert, P.; Nowak, A.; Poschl, U.; Zhu, T.; Hu, M.; Zeng, L. M. *J. Geophys. Res.* **2009**, *114*, D00G10.
(40) Khalizov, A. F.; Xue, H.; Zhang, R. *J. Phys. Chem.* **2009**, *113*, 1066–1074.
(41) Zhang, R. Y.; Khalizov, A. F.; Pagels, J.; Zhang, D.; Xue, H. X.; McMurry, P. H. *Proc. Natl. Acad. Sci. U.S.A.* **2008**, *105*, 10291–10296.
(42) Jacobson, M. Z. *Nature* **2001**, *409*, 695–697.
(43) Zhang, R. Y.; Li, G. H.; Fan, J. W.; Wu, D. L.; Molina, M. J. *Proc. Natl. Acad. Sci. U.S.A.* **2007**, *104*, 5295–5299.
(44) Zuberi, B.; Johnson, K. S.; Aleks, G. K.; Molina, L. T.; Laskin, A. *Geophys. Res. Lett.* **2005**, *32*, L01807.

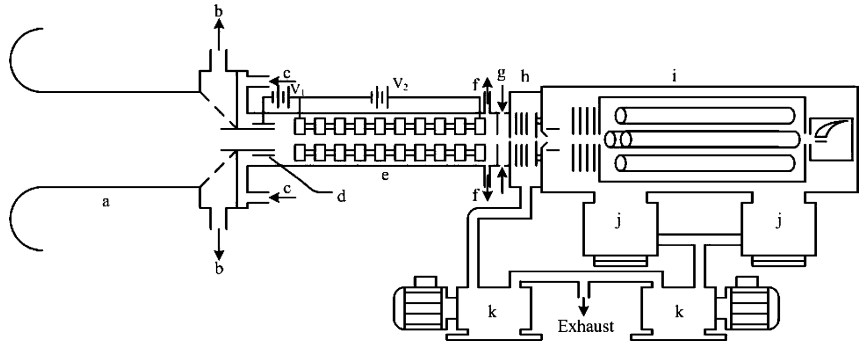

Figure 1. Schematic diagram of the AP-ID-CIMS: (a) 4-in. ID inlet; (b) flow to sampling blower; (c) 10 slpm N_2 carrier doped with HNO_3 and C_3H_8; (d) Am-241 holder; (e) atmospheric pressure drift tube; (f) 65 slpm drift tube flow, including 10 slpm N_2 carrier flow, pumped by a diaphragm pump, and regulated by a mass flow controller; (g) 400 sccm N_2 curtain flow to prevent water clusters formation; (h) CID chamber; (i) quadrupole mass spectrometer;(j) turbo pumps; (k) oil pumps for rough pumping.

of the inlet (denoted as dash lines in Figure 1a). A flow of about 55 slpm from the total sample flow is introduced into the drift tube by a diaphragm pump through a 0.75-in ID 1.5-in long stainless steel tube, around which is another 1-in ID 0.5-in long stainless steel tube holding the ion source made from a 0.4-in ×3-in Am-241 foil (NRD). Near 10 slpm pure N_2 doped with HNO_3 vapor (a few parts per million by volume, ppmv) from a 70% HNO_3 solution (Sigma-Aldrich, >99.99%) and ~230 ppmv propane (Matheson Tri-Gas, >99.9%), an OH radical scavenger, pass through the ion source to carry the produced reagent ions, $NO_3^-\cdot(HNO_3)_{n=0,1,2}$, into the drift tube region. The number of HNO_3 ligands attached to the NO_3^- ions depends on the concentration of HNO_3 within the N_2 carrier gas. Under typical operating conditions of our instrument, $NO_3^-\cdot HNO_3$ is the most abundant reagent ion. The gap between the ion source holder and the drift tube inlet forms a sheath flow to prevent ambient air from being radiated by the Am-241. The drift tube is 7.5-in. long and consists of twenty 1.5-in. i.d. alternate stainless steel and Teflon rings. The steel rings are interconnected by 2 MΩ resistors with the last one grounded. A potential of −17 V relative to the first ring is applied to the ion source to repel negatively charged reagent ions into the drift tube and to increase the intensities of both reagent and product ions. A potential of −168 V is applied to the front ring of the drift tube, and an electric field of −8.8 V cm^{-1} is developed along the center of the drift tube. As guided by the electric field, NO_3^- core ions react with H_2SO_4,

$$NO_3^-\cdot(HNO_3)_n + H_2SO_4 \rightarrow HSO_4^-\cdot(HNO_3)_n + HNO_3 \quad \text{(R1)}$$

Figure 2 shows the mass spectrum of both NO_3^- and HSO_4^- core ions detected at m/e = 62 (NO_3^-), 125 ($NO_3^-\cdot HNO_3$), 188 ($NO_3^-\cdot(HNO_3)_2$), 97 (HSO_4^-), and 160 ($HSO_4^-\cdot HNO_3$). The collision-limited rate constant (k_1) for reaction R1 (n = 1) at 300 K is 1.86×10^{-9} cm^3 s^{-1} (ref 45). To prevent ambient water vapor from entering the CID chamber and causing formation of water clusters, a 0.25-in. long curtain flow chamber is installed immediately after the drift tube. About 400 standard cubic centimeters per minute (sccm) of dry N_2 is supplied into

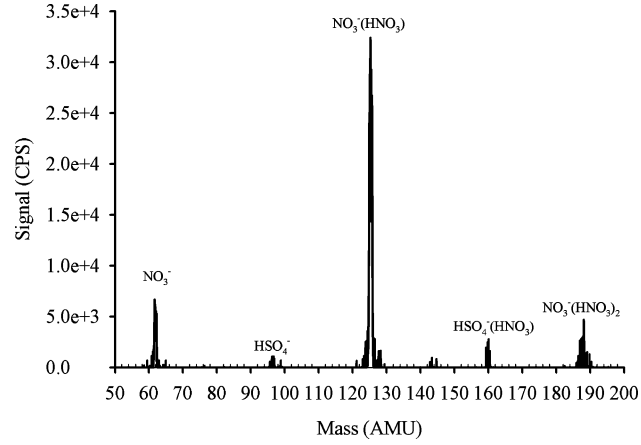

Figure 2. Mass spectrum of the reagent ions and the product ions.

the curtain chamber (Figure 1g), most of which is pulled into the drift tube through a 0.1-in. diameter aperture. The curtain flow chamber is biased at 7 V, assisting ions to penetrate the dry N_2 flow. The CID chamber is 1-in. long and houses four evenly spaced electrostatic lenses. The pinhole size in front of the CID is 200 μm, and the operating pressure in the CID is maintained at ~0.6 Torr by an oil vane pump (Edwards, E2M30). At the end of the CID, an 800 μm pinhole leads the ionic species to the quadrupole mass spectrometer (QMS, ABB Extrel QC-150). The QMS is differentially pumped by two Varian TV551 turbo pumps and detects up to 500 atomic mass unit (amu).

Quantification of H_2SO_4 by AP-ID-CIMS. In a conventional flow tube configuration, ions move freely with the carrier gas and ion diffusion potentially scatters the ion cloud and some ions discharge at the wall surface.[15] Inside the drift tube, however, ions are under influence of an electric field along the axial direction, and their flight paths are well under control. The working principle of the AP-ID-CIMS is similar to the ID-CIMS.[18] H_2SO_4 concentration is determined by

$$[H_2SO_4] = [HSO_4^-\cdot HNO_3]/(k_1 \Delta t [NO_3^-\cdot HNO_3]) \quad \text{(E2)}$$

where Δt is the reaction time inside the drift tube and is calculated from the drift tube length, L, and the apparent velocity of the ions, U, which is the sum of the carrier gas flow velocity, U_f, and the

(45) Viggiano, A. A.; Seeley, J. V.; Mundis, P. L.; Williamson, J. S.; Morris, R. A. *J. Phys. Chem. A* **1997**, *101*, 8275–8278.

ion drift velocity, U_d. U_f is calculated from the carrier gas flow rate and the inner diameter of the drift tube. U_d is determined by equation

$$U_d = \mu_0(760/P)(T/273)E \quad \text{(E3)}$$

where μ_0 is the reduced ion mobility of $NO_3^-\cdot HNO_3$ at 760 Torr and 273 K, E is the electric field strength (-8.8 V cm^{-1} in this work), and P and T are the pressure and temperature inside the drift tube, respectively.

The μ_0 for $NO_3^-\cdot HNO_3$ is calculated according to the equation[15]

$$\mu_0 = \frac{1.85 \times 10^4}{\bar{\Omega}\sqrt{T_{eff}}}\left(\frac{m+M}{mM}\right)^{1/2} \text{cm}^2\cdot\text{V}^{-1}\cdot\text{s}^{-1} \quad \text{(E4)}$$

where T_{eff} is the effective temperature of the carrier gas (in K), m and M are the masses (in atomic mass units) of the ion ($NO_3^-\cdot HNO_3$) and the carrier gas (N_2), respectively, and $\bar{\Omega}$ is the momentum-transfer collision integral (in cm^2). In this work, μ_0 for $NO_3^-\cdot HNO_3$ is determined to be 2.85 cm^2 V^{-1} s^{-1} and the corresponding ionic mobility at 760 Torr and 300 K is 3.11 cm^2 V^{-1} s^{-1}. U_f is about 95.1 cm s^{-1} for a 65 slpm gas flow rate, and U_d is 27.4 cm s^{-1} at one atmosphere pressure and 300 K. The reaction time inside the drift tube is 156 ms (the detailed calculation procedures have been described elsewhere).[17,27] The accuracy of eq E2 depends on several factors, including the uncertainties associated with the mass discrimination of the quadrupole and estimations of the ion-molecular reaction rate coefficient and the reduced ionic mobility and can be evaluated by calibration with primary H_2SO_4 standards.

Calibration of H_2SO_4. Validation of the AP-ID-CIMS methodology requires a primary H_2SO_4 source. In this work, we have developed a device capable of generating variable levels of gaseous H_2SO_4 standards. The device consists of a 184.9 nm UV light source (UVP, 90-0012-01) housed inside a 0.5-in. o.d. 5-in. long stainless steel tube, a 0.25-in. diameter bandpass filter centered at 185 nm with 20 nm bandwidth (OMEGA Optical, XB32), a set of turbulence-inducing fins, and a series of pinholes to control UV flux emitted from the light source. H_2SO_4 standards are generated in situ through reactions R2−R4

$$SO_2 + OH + M \rightarrow HSO_3 + M \quad \text{(R2)}$$

$$HSO_3 + O_2 \rightarrow SO_3 + HO_2 \quad \text{(R3)}$$

$$SO_3 + H_2O + M \rightarrow H_2SO_4 + M \quad \text{(R4)}$$

OH radicals of a known concentration are produced by photodissociation of ambient H_2O vapor at 184.9 nm[29,46]

$$H_2O + h\nu\ (\lambda = 184.9\ \text{nm}) \rightarrow H + OH \quad \text{(R5)}$$

$$H + O_2 \rightarrow HO_2 \quad \text{(R6)}$$

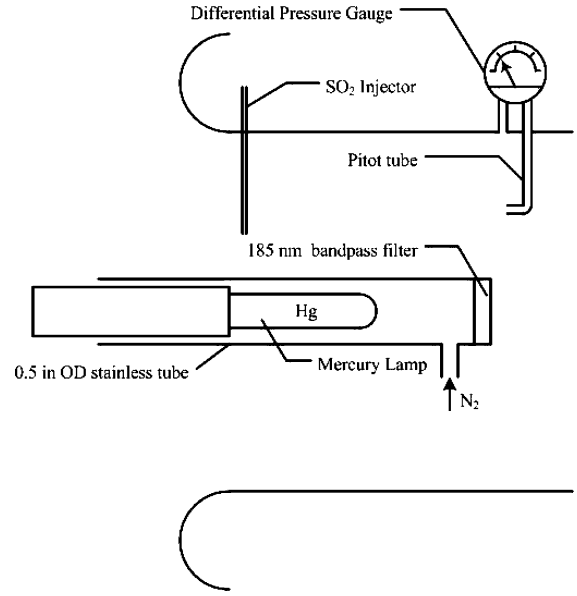

Figure 3. Schematic diagram of the H_2SO_4 calibration device.

Figure 3 shows the UV light source positioned inside the sample inlet. The UV lamp housing is constantly purged with N_2 to prevent O_3 formation. The bandpass filter removes 254 nm emissions from the mercury lamp and avoids photolysis of ambient O_3. To convert OH into H_2SO_4, a flow of 8 sccm SO_2 (Sigma-Aldrich, >99.9%) is injected into the inlet and mixed with the sample air stream to achieve a final concentration of about 7 ppmv, which efficiently ($t_{1/2} \approx 2$ ms) converts all OH radicals into H_2SO_4. As an OH scavenger, another flow of about 10 sccm propane (Matheson Tri-Gas, >99.9%) is introduced into the drift tube region through a nitrogen carrier flow (Figure 1c), with a final mixing ratio of 230 ppmv to terminate possible chain reactions initiated by OH radical produced from the oxidation of ambient NO into NO_2 by HO_2 generated from either reaction R3 or R6. Two propeller-shaped fins serve as the turbulizer to evenly distribute H_2SO_4 in the radial direction. The concentration of the H_2SO_4 standard is determined by

$$[H_2SO_4] = I_{184.9}t\sigma_{H_2O}\phi_{H_2O}[H_2O] \quad \text{(E5)}$$

where $I_{184.9}$ is the 184.9 nm photon flux, t is the illuminating time, σ_{H_2O} is the absorption cross section of H_2O at 184.9 nm ($= 5.5 \times 10^{-20}$ cm^2 (ref 47)), ϕ_{H_2O} is the quantum yield of photodissociation of H_2O (= 1), and $[H_2O]$ is the water vapor number concentration in the sample air. $[H_2O]$ is measured by a commercial hygrometer (Edge Tech, Dew Prime II). The time (t) is determined from the airflow velocity inside the inlet that is measured by a built-in Pitot tube and a differential pressure gauge (Dwyer model 2000). $I_{184.9}$ is measured by a solar blind CsI photocathode (Hamamatsu R5764), and its sensitivity at 184.9 nm is certified by the National Institute of Standards and Technology (NIST). Because of the strong absorption of O_2 at 184.9 nm, $I_{184.9}$ attenuates exponentially along the UV light path. For a distance of 15 cm away from the lamp housing, $I_{184.9}$ is less than 1.5% of the value measured

(46) Berresheim, H.; Elste, T.; Plass-Dulmer, C.; Eisele, F. L.; Tanner, D. J. *Int. J. Mass Spectrom.* **2000**, *202*, 91–109.

(47) JPL. *Chemical Kinetics and Photochemical Data for Use in Atmospheric Studies*; Evaluation 15; NASA, JPL, Caltech: Pasadena, CA, 2006.

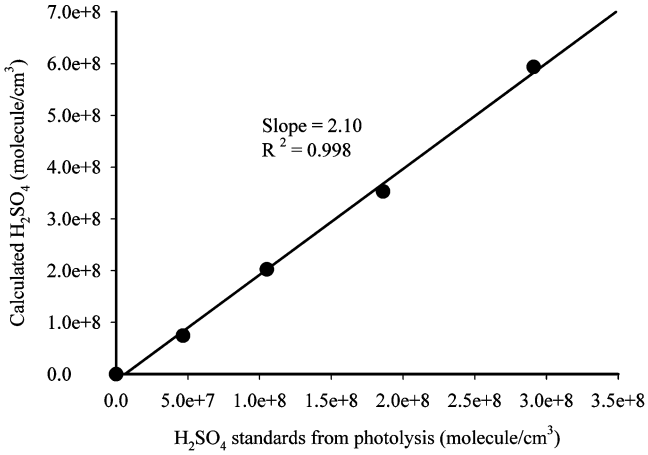

Figure 4. Correlation between H_2SO_4 concentration calculated directly from measured analyte and reagent ion intensities according to E2 and H_2SO_4 concentration calculated from photolysis rate according E5 with the primary standards corresponding to orifice sizes of 0.0, 2.0, 3.0, 4.0, and 5.0 mm, respectively.

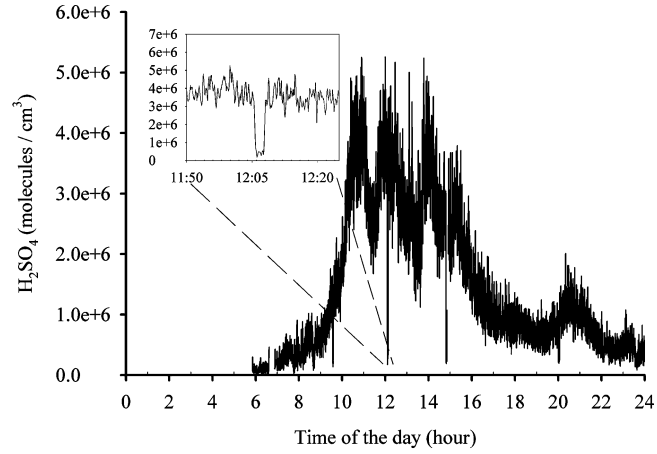

Figure 5. H_2SO_4 time series measured on Feb 19, 2008. In the early morning, it was clear and mostly ESE wind. Around 10:50, cloud started building up and wind direction switched from ESE to SE. Backgrounds were checked at 6:40, 9:30, 12:06, 14:45, and 20:05.

immediately in front of the light source. To precisely obtain the spatial profile of $I_{184.9}$, the light source and the photocathode are mounted on a 2-dimension (2-D) graduated framework. The light source is treated as the origin of a Cartesian coordinates. By moving the photocathode away from the light source at a 0.5-cm increment in both X and Y directions, $I_{184.9}$ is mapped onto a 5-cm ×15-cm 2-D surface with a grid size of 0.5-cm ×0.5-cm. The total 184.9 nm photon flux inside the 4-in ID cylindrical illuminated area is obtained from integration of the 2-D grid measurements along the radial direction.

RESULTS AND DISCUSSION

Laboratory Evaluation. In principle, the AP-ID-CIMS is able to quantify analytes using reagent/product ion intensities, ion−molecule reaction rate constant, and reaction time, as described by eq E2. The accuracy in the quantification of neutral species is dependent on several parameters used in the calculation, such as the quadrupole transmission efficiency, the ion−molecule reaction rate constant, and the reduced ionic mobility. Using the calibration device described above, we have conducted multiple-point calibration by adjusting the UV radiation intensity with a series of pinholes (5, 4, 3, 2, and 0 mm). The generated H_2SO_4 concentration typically ranges from 10^7 to 10^8 molecules cm^{-3}. Figure 4 shows the correlation between calculated H_2SO_4 concentrations with the primary H_2SO_4 standards determined from eq E5. The slope of the linear regression is 2.1, corresponding to a calibration factor that can be used to correct the calculation in field measurements. Such a result also implies a high efficiency for the combined ionization/transmission/detection from the inlet to detector. For a 12 s integration time, the sensitivity of the AP-ID-CIMS is about 5×10^4 molecules cm^{-3} per cps.

To further demonstrate the advantage of the AP-ID setup, we have compared the performance of the AP-ID-CIMS with the flow tube AP-CIMS setup, in which the drift tube is replaced by a 7.5-in. long 1.5-in. i.d. Pyrex glass tube with an aluminum mesh lining. The mesh is grounded to prevent charge buildup on the glass surface, whereas the remaining configuration is kept similarly. The results show that when an identical amount of gaseous H_2SO_4 is measured by both the AP-ID-CIMS and the flow tube AP-CIMS, the signal-to-noise ratio increases by a factor of 3 in the former case. Other AP-CIMS applications have previously been reported in the literature.[16]

Field Evaluation. To demonstrate that the AP-ID-CIMS is capable of in situ detection of ambient H_2SO_4, a field evaluation has been conducted on a rooftop of a thirteen-floor building on the campus of Texas A & M University (30.61° N, −96.32° W). The AP-ID-CIMS was in operation from February 19 to April 14, 2008, excluding rainy and cloudy days. Some nighttime measurements were also conducted. The QMS was set to integrate $HSO_4^-\cdot HNO_3$ signal for about 12 s and collect the $NO_3^-\cdot HNO_3$ signal for 50 ms every 12 s. Mass spectrum scans were conducted periodically to check the QMS performance.

Figure 5 depicts the H_2SO_4 time series observed on February 19, 2008. H_2SO_4 increased rapidly after 9:00 Central Standard Time (CST) and reached near 5.4×10^6 molecules cm^{-3} at 10:15. From 11:00 to 15:00, the concentration of H_2SO_4 showed a significant fluctuation concurring with variations in the cloud coverage. Daytime backgrounds were obtained by applying a single layer of Nylon cloth coated with sodium bicarbonate to the 0.75-in. drift tube inlet (Figure 1). The insert in Figure 5 corresponds to a background check at 12:06, showing that H_2SO_4 immediately dropped to about 3×10^5 molecules cm^{-3} when the Nylon cloth was applied and quickly recovered after removing the Nylon cloth. Backgrounds were also checked at 9:30, 14:45, and 20:05. After sunset, a small peak was observed around 20:30 that might be the result of an air parcel with residual H_2SO_4.

Figure 6 shows H_2SO_4 time series measured on four selected days, that is, March 21 and 22 and April 11 and 13, 2008. On March 21, there was a black smoke event occurring about 9:00, originated from a fire fighter training site about 1 mile to the SSE of the observation site. The arrow in Figure 6a indicates the period when the smoke covered the observation site and clearly a delayed increase in the H_2SO_4 time series was recorded during this event. H_2SO_4 increased quickly after 9:15 when it was clear and reached about 1.2×10^7 molecules cm^{-3} around 10:40. When clouds started building up, H_2SO_4 decreased

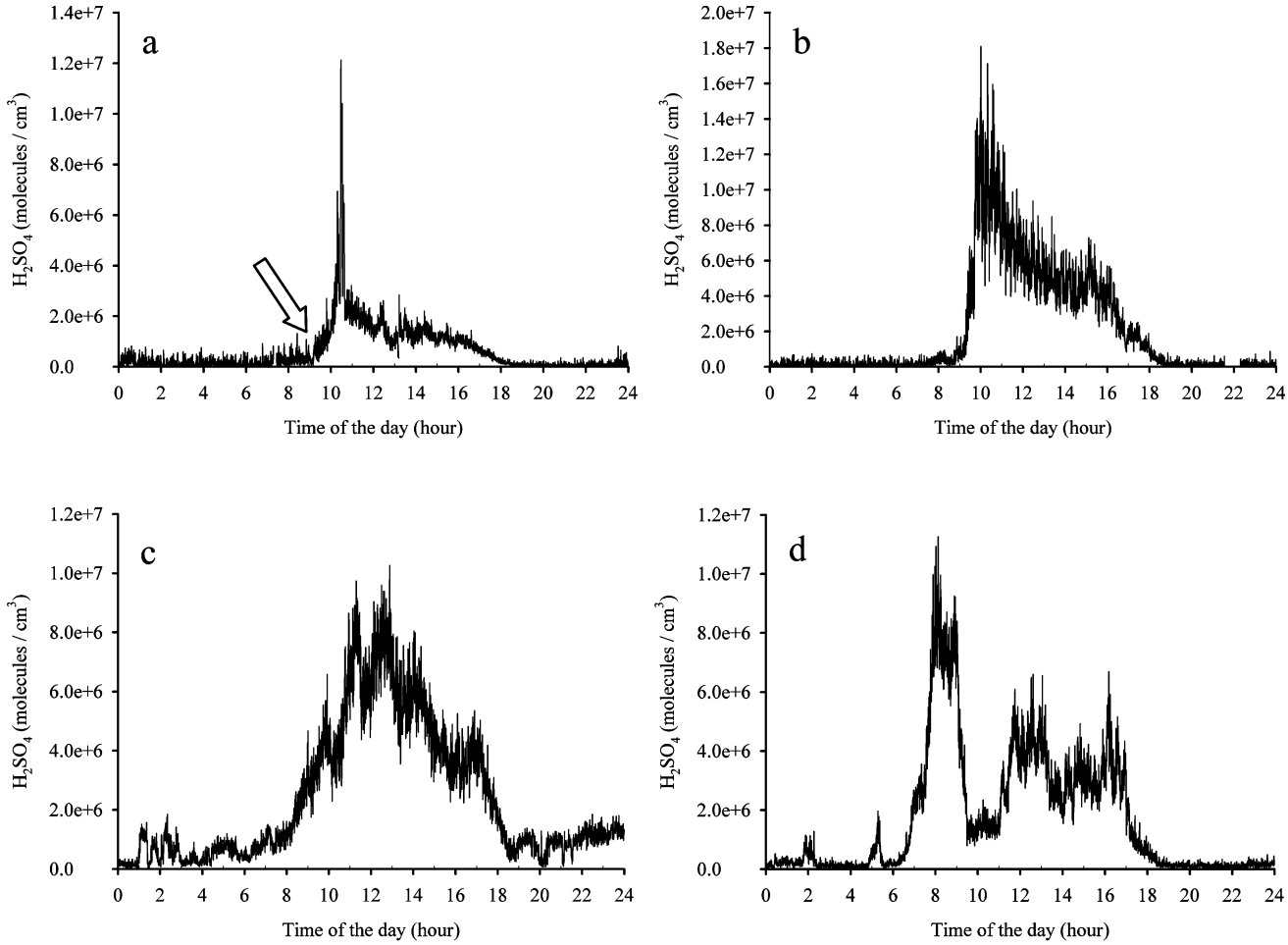

Figure 6. H_2SO_4 profile observed on (a) March 21, (b) March 22, (c) April 11, and (d) April 13, 2008. The arrow in (a) indicates a black smoke event originated from a nearby fire fighter training site. On March 21, it was mostly clear in the early morning and then became partly cloudy. After 10:40, clouds continued building up and after 12:00, it became mostly cloudy for the rest of the day. South wind persisted the whole day with gusts of more than 20 mph. March 22 was mostly clear with persisting south wind. April 11 was characterized by a strong north wind (~12 mph) and low relative humidity (52% at 7:00). On April 13, 2008, it was mostly clear and characterized by a dry and cold weather pattern. The site also experienced gusty wind after 9:00 with the maximum speed of ~28 mph. Wind direction was mostly from north in the early morning, switched to NE around 9:00, and then switched to NW after 11:00.

significantly and remained below about 2.0×10^6 molecules cm^{-3} after 11:00, and H_2SO_4 decreased below detection limit before sunset.

Figure 6b shows that, on March 22, H_2SO_4 increased rapidly after 9:30 and reached a maximum value of 1.7×10^7 molecules cm^{-3} at about 10:00, the highest H_2SO_4 concentration observed during the field evaluation. Figure 6c shows the H_2SO_4 profile measured on April 11, 2008, clearly following the solar cycle. The lifetime of sulfuric acid molecules in the atmosphere depends on pre-existing aerosol surface area. Given an average aerosol surface area in the urban area (~800 μm^2 cm^{-3}) and an uptake coefficient of 0.73 (ref 48), the lifetime of H_2SO_4 is about 27 s. Lingering nighttime H_2SO_4 was also evident and might originate from some nonphotochemical H_2SO_4 formation mechanism, such as ozonolysis of alkene species,[49,50] as has been observed elsewhere.[28] On April 13, 2008 (Figure 6d), H_2SO_4 profile shows influence from the fluctuation in wind direction.

The detection limit for H_2SO_4 during the field evaluation is estimated to be less than 10^5 molecules cm^{-3} on the basis of 3σ of the background noise, which is improved over the conventional ID-CIMS system operating at a lower drift tube pressure (<3 Torr). For example, the detection limits of HNO_3 and N_2O_5 using an ID-CIMS are about 38 and 30 pptv, corresponding to 9×10^8 and 7×10^8 molecules cm^{-3}, for 5-min and 10-s average time, respectively, based on three times the standard deviation of the baseline signals for measurements made in an urban environment.[27] Such a substantial improvement in the detection sensitivity is largely attributed to the use of atmospheric pressure drift tube, which enables a significantly longer ion−molecule reaction time and eliminates dilution of ambient samples, in addition to providing a well-defined electric field with the benefits to confine the flight path and velocity of reagent ions, to break down ion clusters, and to have a well-defined ion−molecule reaction time. The background noise used to calculate the detection limit is taken from nighttime observation with nylon cloth, which is much lower than daytime measurement. The daytime background checks shown in

(48) Jefferson, A.; Eisele, F. L.; Ziemann, P. J.; Weber, R. J.; Marti, J. J.; McMurry, P. H. *J. Geophys. Res.* **1997**, *102*, 19021–19028.
(49) Fan, J.; Zhang, R. *Environ. Chem.* **2004**, *1*, 140–149.
(50) Zhang, D.; Lei, W. F.; Zhang, R. Y. *Chem. Phys. Lett.* **2002**, *358*, 171–179.

Figure 5 are conducted with one layer of nylon cloth to test the performance of the AP-ID-CIMS, while maintaining the large volume flow rate. Thus, the daytime background checks do not represent a typical background contamination level of the instrument. Our measured ambient H_2SO_4 variations by the AP-ID-CIMS are consistent with previous observations under similar environment.[28,29] The accuracy of ambient H_2SO_4 measurements is determined by the parameters to calculate the absolute H_2SO_4 standard concentration. The parameters, $I_{184.9}$, t, and $[H_2O]$, can be measured with good accuracy (uncertainty <2%). The absorption cross section of water at 184.9 nm is taken from literature, with a value of 5.5×10^{-20} cm^2 (ref 47). However, Cantrell et al.[51] reported a value of 7.14 ($\pm$0.2) $\times 10^{-20}$ cm^2 at 25 °C, with a small positive temperature dependency (4% from 0 to 80 °C). In addition, Parkinson and Yoshino[52] obtained a value of 7.0×10^{-20} cm^2 at 22 °C. Hence, the most uncertain parameter is the water absorption cross section. We estimate that the uncertainty in H_2SO_4 measurements should be less than 16%, if the average of the literature values is adopted in eq E5.

CONCLUSION

We have developed an atmospheric pressure-ion drift tube and demonstrated its application for ambient H_2SO_4 measurements. Operation of the drift tube at atmospheric pressure allows a longer ion−molecule reaction time and eliminates dilution of ambient samples, while a well-defined electric field inside the drift tube provides the advantages to confine the flight path and velocity of reagent ions, to break down ion clusters, and to control the ion−molecule reaction time. Through ab initio quantum chemical calculation,[27] we have estimated the reduced ionic mobility of the reagent ion, $NO_3^-\cdot HNO_3$, allowing quantification of the H_2SO_4 concentration without on-site calibration. To evaluate the uncertainties associated with parameters used in the calculation, a primary H_2SO_4 source has been developed to generate H_2SO_4 standards with variable concentrations. The AP-ID setting effectively constrains the ion flight path and minimizes ion wall losses inside the drift tube, improving the sensitivity by a factor of 3 over the conventional flow tube AP-CIMS setup. The detection sensitivity of AP-ID-CIMS is improved by 3 orders of magnitude over the low-pressure ID-CIMS, because of a longer ion−molecule reaction time and no dilution of ambient samples. A field evaluation of the AP-ID-CIMS shows that H_2SO_4 diurnal profiles vary with cloud coverage and wind direction and speed and indicate that the ambient H_2SO_4 level is controlled by photochemical production and condensation sinks. In this work, we have demonstrated the application of the AP-ID-CIMS using gaseous H_2SO_4 as an example, since detection of sulfuric acid is extremely challenging because of its low atmospheric concentration and sticky nature. Using appropriate ion-molecule reaction schemes, the AP-ID-CIMS technique can potentially be used to improve detection of other atmospheric organic and inorganic trace gases.[13,27]

(51) Cantrell, C. A.; Zimmer, A.; Tyndall, G. S. *Geophys. Res. Lett.* **1997**, *24*, 2195–2198.
(52) Parkinson, W. H.; Yoshino, K. *Chem. Phys.* **2003**, *294*, 31–35.

ACKNOWLEDGMENT

This work was supported by the Robert A. Welch Foundation (Grant A-1417) and the U.S. National Science Foundation (AGS-0938352 and CBET-0932705). R.Z. acknowledges further support from the National Natural Science Foundation of China Grant (40728006).

Received for review May 12, 2010. Accepted July 27, 2010.

AC101253N